Anal. Bioanal. Electrochem., Vol. 16, No. 8, 2024, 728-736
https://www.doi.org/10.22034/abec.2024.715423

Analytical & Bioanalytical Electrochemistry

Full Paper

Synthesis and Characterization of Tetraaza-Macrocyclic Complexes of Mn^{II} and Ni^{II}: Electrochemical and Antibacterial Evaluation

Vinod Kumar Vashistha,[1,*] Dipak Kumar Das,[2] Bhaskar Vallamkonda,[3] and Suman Yadav[4]

[1]*Department of Chemistry, University of Lucknow, Lucknow-226007, India*
[2]*Department of Chemistry, GLA University, Mathura-281406, India*
[3]*Department of Pharmaceutical Science, VIGNAN'S Foundation for Science, Technology & Research, Vadlamudi, Guntur-522213, Andhra Pradesh, India*
[4]*Department of Chemistry, Swami Shraddhanand College, University of Delhi, Delhi-110036, India*

*Corresponding Author, Tel.: +91-8266807046
E-Mails: vkviitr@gmail.com ; vkv.uol@gmail.com

Received: 28 March 2024 / Received in revised form: 15 July 2024 / Accepted: 20 August 2024 / Published online: 31 August 2024

Abstract- Macrocyclic complexes play a crucial role in various emerging fields, including electrocatalysis, catalysis, sensor technology, pharmaceuticals, and biological applications. In this study, we synthesized a tetraaza-macrocyclic cavity capable of hosting transition metals, specifically Mn^{II} and Ni^{II}, forming the MnN_4 and NiN_4-macrocyclic complexes, respectively. Structural analyses were performed to propose the configuration of these complexes. Additionally, electrochemical studies were conducted to assess their redox potential and electron transfer kinetics. Furthermore, the biological activity of the complexes as antibacterial agents against a broad spectrum of microorganisms was investigated. The findings revealed that these complexes exhibit favorable redox properties with rapid electron transfer kinetics. The cyclic voltammogram was showed interesting results by eliminating ligand oxidation redox couple were observed as comparable in DMSO with shifting of 0.13 V peak potential in -ve peak potential range with the decreament in peak height. These results underscore the multifaceted applications of tetraaza-macrocyclic complexes in diverse fields, highlighting their importance in both fundamental research and practical biomedical interventions.

Keywords- Cyclic voltammetry; Metal complexes; biological study; Mn^{II}; Ni^{II}; Tetraaza-macrocycle

1. INTRODUCTION

While the globe struggles to fight the coronavirus pandemic (COVID-19), an even bigger risk of antimicrobial resistance is looming in the shadows. Antimicrobial resistance is concerning with microorganisms because bacterial resistance thrives in hospitals and health centers, placing all individuals at risk regardless of the intensity of their medical illnesses, and complicating COVID-19 management [1]. Antimicrobial resistance is an exceedingly important hazard to public health worldwide, necessitating creative methods to combat newly arising and widely disseminating defense mechanisms in contagious organisms [2]. Macrocyclic Schiff base analogues work well as chelating agents and are capable of forming a variety of metal complexes [3]. The stability of Schiff base ligands is frequently increased by complex formation with metal, and numerous macrocyclic complexes have also been observed to be more highly stable than equivalent species with acyclic ligands from a thermodynamic and kinetic perspective [4].

Additionally, advances in synthetic macrocyclic chemistry have led to a better appreciation of the characteristics and purposes of biological macrocycles and their complexes that are found in nature [5]. Macrocyclic complexes have earned a lot of interest since they are engaged in critical biochemical functions including photosynthesis and dioxygen transportation, as well as possess good antimicrobial activities [6].

Tetraazamacrocyclic ligands can be easily synthesized by the condensation of dicarbonyl and primary amine which play a key factor in the creation of macrocyclic ligands [7]. Macrocyclic compounds of transition-metal with tetraaza groups have been used as prototypes to meet the requirements and oxygen carrier systems have several intriguing characteristics and biological roles [8,9] thus macrocyclic chemistry has dramatically advanced [10,11]. As metal complexes work similarly to porphyrin counterparts in catalyzing chemical processes, tetraaza macrocyclic ligands are interesting. The effective nuclease activity of macrocyclic complexes has been discovered [12,13], motivating inorganic chemists to look for novel metal complexes for bioactive molecules. Metal complexes are extremely valuable in biological activities attributable to their unique characteristics [12,14]. In recent years, macrocyclic complexes of Mn [15-21] and Ni [22-25] have been investigated for their antimicrobial potency.

In this work, we carried out the synthesis of Schiff's base by the reaction of 2, 3-diamino naphthalene and 2, 6-diethylcarboxylate followed by its complexation with Mn (II) and Ni (II). The tetrazamacrocyclic complexes were characterized by employing multiple analytical technologies. The synthesized complexes were undergone electrochemical studies to evaluate their redox potential and electron transfer kinetics, and their antimicrobial activities.

2. EXPERIMENTAL SECTION

2.1. Materials and methods

Naphthalene and 2,6-diethyl carboxylate were obtained from Merk (Mumbai, India). The details of the equipment used in the present study are as follows:

- Microanalysis: Eager Xperience elemental analyzer, Thermo Fisher Scientific Inc. USA.
- Mass spectra: TOF MS ES+6018e3 mass spectrometer.
- IR spectra: Schimadzu 8400S spectrometer using KBr DRS system
- UV-vis spectra were recorded on Schimadzu 2450 spectrophotometer
- Conductivity measurement: Auto-ranging Conductivity/TDS Meter (TCM^{+})
- Cyclic voltammetry: Metrohm Model 663VA Stand potentiostat/galvanostat, Pt disc as working electrode, Pt wire as counter electrode, and Ag/AgCl (saturated KCl) as the reference electrode

2.2. Synthesis of Schiff base tetraazamacrocyclic complexes

To carry out the synthesis of two Schiff base tetraazamacrocyclic complexes, the template method was employed. The brief procedure is as follows: to a solution of 2,3-diamino naphthalene (DAN) in methanol (0.002 mol), 2,6-diethyl carboxylate (DEC) (0.002 mol) was slowly added in a round bottom flask. The condensation between DAN and DEC resulted in to formation of Schiff's base macrocyclic ligand. The resulting mixture was then treated with a methanolic solution of $MnCl_2.4H_2O$ (0.001 mol) and $NiCl_2.6H_2O$ (0.001 mol) and refluxed for 8 hrs, the dark brown and brown colored powders were obtained, respectively, and recrystallized in the mother liquor.

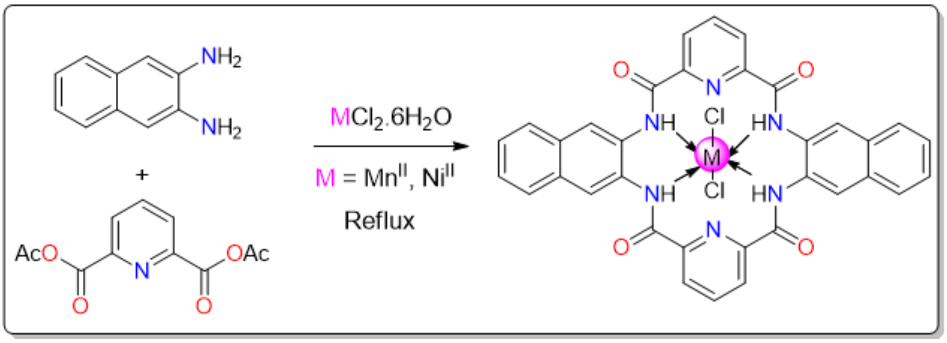

Figure 1. Reaction for the synthesis of metal complexes of Mn^{II} and Ni^{II}

3. RESULTS AND DISCUSSION

3.1. Physical properties

The color of Schiff's base MN_4 complexes of Mn^{II} and Ni^{II} are dark brown and pale brown, respectively. Both complexes were discovered to be soluble in solvents such as methanol (MeOH), N, N-dimethylformamide (DMF), dichloromethane (DCM), and acetonitrile (ACN).

The complexes were non-hygroscopic and stable at room temperature. Molecular mass analysis revealed that the complexes were monomeric in structure. The complexes were non-electrolytic, as indicated by the molar conductance determination. As a result, this formula of complexes can be written as $[M(L)X_2]$, where M = Mn^{II}, and Ni^{II}. The physical and analytical data are presented in Table 1.

Table 1. Physical and analytical data of MnN_4 and NiN_4 complexes

Complex	**Yield**	**M.P.**	**Color**	**M.W Found (calc.)**	**Elemental analysis; Found (calc.) in %**			**Molar cond.**
					C	**H**	**N**	
$[C_{34}H_{22}N_6O_4Mn]Cl_2$	75.28	190	Green	688 (704)	56.88 (57.59)	3.01 (3.12)	11.90 (11.93)	32
$[C_{34}H_{22}N_6O_4Ni]Cl_2$	90.80	180	Brown	701 (707)	57.65 (57.70)	3.10 (3.11)	11.86 (11.88)	40

3.2. Spectral studies

3.2.1 UV/Vis Spectra

Electronic spectral studies of Mn/Ni-N_4 complexes of Mn^{II} and Ni^{II} were recorded in 0.001 M methanolic solution of the complexes. The spectra of the Mn-N_4 complex displayed absorbance signal in the range of 15,869−16,739 cm^{-1} (ε_{max}= 61−64 L. mol^{-1}. cm^{-1}), 20,351−21,681 cm^{-1} (ε_{max}=32−35 L·mol^{-1} cm^{-1}), 24,785-27,001 cm^{-1} (ε_{max}= 60−63 L. mol^{-1}·cm^{-1}), which could be allocated to $^6A_{1g}$ – $^4A_{1g}$ (4G), $^6A_{1g}$ - ^4E_g, $^6A_{1g}$ (4G) (10B + 5C), $^6A_{1g}$ – ^4E_g (4D) (17B + 5C) and $^6A_{1g}$ – $^4T_{1g}$ (4P) transitions, correspondingly.

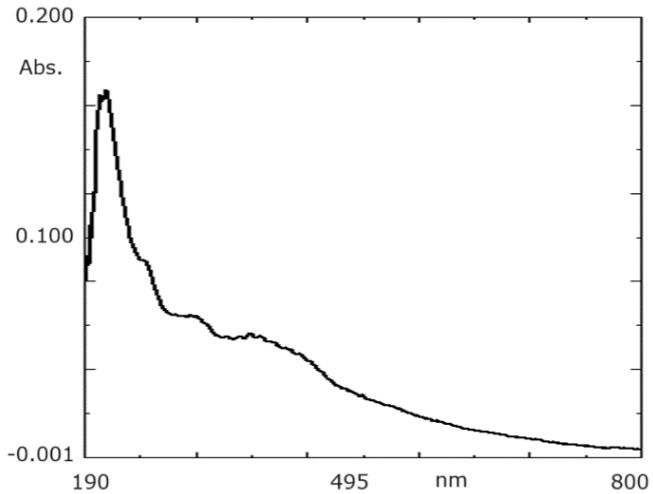

Figure 2. UV-vis spectra of MnN_4 complex in 0.001 M methanolic solution of complex

Likewise, the UV spectra Ni-N_4 (II) complex show three absorption bands in the range 17,384−18,434 cm^{-1} (ε = 70-84 $L \cdot mol^{-1} \cdot cm^{-1}$), 18,719−19,128 cm^{-1} (ε = 44−58 $L \cdot mol^{-1} \cdot cm^{-1}$) and 22,565−24,418 cm^{-1} (ε = 129−132 $L \cdot mol^{-1} \cdot cm^{-1}$). Based on this observation a deformed octahedral geometry could be offered to the MN_4 complexes.

3.2.2 IR Spectra

Infra-red spectra of two MN_4 complexes demonstrated a medium intensity band in the range 3200-3300 cm^{-1}. These bands could be assigned to NH stretching due to the amide group present in the ligand structure. Peaks in the range 1600-1630 cm^{-1} correspond to C=N stretching mode which supports the presence of amidic bond in the complex. The moderate-intensity bands in the 2820-2950 cm^{-1} range are caused by C-H stretching modes. Additional bands in the region 430-480 cm^{-1} are due to the M-N stretching mode indicating the presence of the M-N bond in the complex. The IR spectrum of the NiN_4 complex is shown in Figure 3.

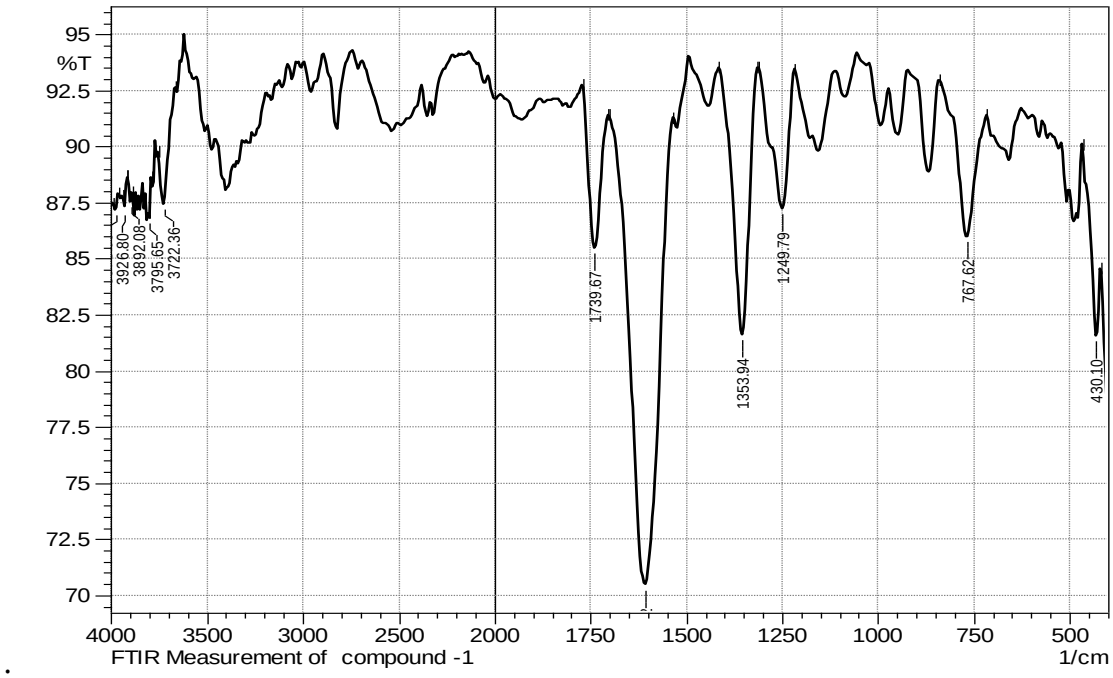

Figure 3. IR spectra of Ni-N_4 complex

3.3. Cyclic voltametric studies

MN_4 macrocyclic complexes were electrochemically studied in various solvents such as DMSO and DMF using 0.1 M TEAP as a supportive electrolyte. The scan rate was kept between 50 and 200 mVs^{-1}. The cyclic voltammogram (Figure 4a) of the Mn^{II} complex was obtained in DMSO solvent at 100 mVs^{-1} scan rate and revealed two anodic peaks matching cathodic peaks in the range of -0.7 V to +0.7 V. Based on peak separation ΔE = 0.10 – 0.17 V

and peak current ratio (i_{pa}/i_{pc} = 1), both the corresponding redox process is observed as quassi-irreversible that could be allocated to $Mn^{+3/+2}$ and $Mn^{+1/+2}$ oxidoreduction course, correspondingly. There are two redox couples are also observed in both positive and negative potential regions with the formal potential at +1.02 V and -1.04 V due to $L^{0/+1}$ and $L^{0/-1}$, correspondingly. Furthermore, the CV plot (Figure 4) of the MnN_4 complex was also observed in DMF under identical circumstances. This cyclic voltammogram was showed interesting results by eliminating ligand oxidation redox couple that were observed as comparable in DMSO with shifting of 0.13 V peak potential in -ve peak potential range with the decrement in peak height.

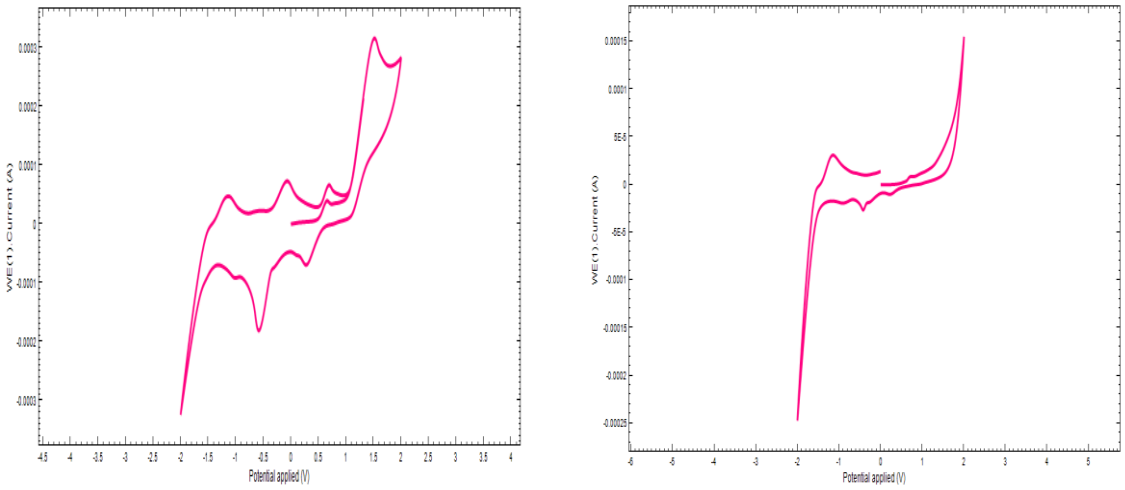

(a) **(b)**

Figure 4. CV plots of Mn^{II} complex in (a) DMSO and (b) DMF containing 0.1 M TEAP recorded at 100 mVs^{-1}

Under identical conditions, the CV plot of NiN_4 complex was observed in DMSO and DMF. This compound exhibited one redox step in DMSO, comparable to the Ni^{+}/Ni^{2+} pair. With the ΔE value of 0.14 V and a peak current ratio i.e. (i_{pa}/i_{pc} = 1), this redox cycle is quasi-reversible. A distinct cathodic peak is also found in the positive potential region, which may be assigned to the $Ni^{+2} \rightarrow Ni^{+}$ reduction process at +0.41 V, whereas in DMF, this complex displayed just one redox process, similar in DMSO, however the peak height is lower. Furthermore, the graphs of i_p versus $v^{1/2}$ for the Mn^{+}/Mn^{+2} and Ni^{+2}/Ni^{+1} oxidative events in both solvents were observed to be linear, showing that these oxidative operations were regulated by diffusion using the Randles-Sevcik equation for reversible electrochemical processes. The theoretical values of diffusion coefficient (D_0) and heterogeneous electron transfer rate constant (K_0) for the Mn^{+}/Mn^{+2} and Ni^{+2}/Ni^{+1} redox pairs in both solvents were computed utilizing Nicholson and Kochi techniques at 100 mVs^{-1} scan rate (Table 2).

Table 2. Heterogeneous rate constant and diffusion coefficient of these macrocyclic complexes Mn^{II} and Ni^{II} at 100 mVs^{-1}

Complexes	**$K_0\times10^{-3}$ (cm/s)**		**$D_0\times10^{-6}$(cm^2/s)**	
	DMSO	DMF	DMSO	DMF
$[C_{34}H_{22}N_6O_4Mn]\ Cl_2$	2.14	1.81	4.49	2.81
$[C_{34}H_{22}N_6O_4Ni]\ Cl_2$	1.96	1.39	2.49	1.14

3.4. Biological activity

An agar well diffusion process was employed to assess the antibacterial properties of MN_4 complexes. DMSO solvent and Gentamycin were served as -ve and +ve control. The antimicrobial properties of both MN_4 complexes were assessed by evaluating the growth of the inhibition zone versus *E. coli*, *S. aureus*, *B. subtilis*, *P. aeruginosa pathogens*, and *C. albicans*. The successful results of antimicrobial studies of two complexes against various microbes are presented in Table 3. The Mn^{II} complex inhibited *E. coli* the most (22 mm), whereas the Ni^{II} complex inhibited *S. aureus* the most (19 mm) (Figure 5).

Table 3. Antimicrobial activity of Mn^{II} and Ni^{II} complexes

Complex (100 mg/ml)	**Diameter of inhibition zone (mm)**				
	E. coli	***P. aeruginosa***	***B. ceureus***	***S. aureus***	***C. albicans***
$[C_{34}H_{22}N_6O_4Mn]Cl_2$	22	18	16	17	19
$[C_{34}H_{22}N_6O_4Ni]Cl_2$	17	12	14	21	16
Gentamycin	24	24	24	24	20

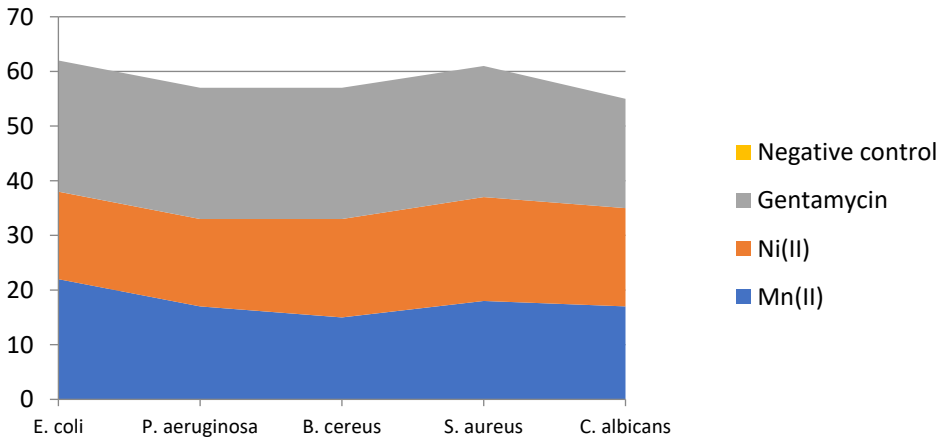

Figure 5. Graphical representation of the antimicrobial activity of Mn^{II} and Ni^{II} Schiff base tetraazamacrocyclic complexes

4. CONCLUSION

In this work, Mn^{II} and Ni^{II} complexes were prepared by condensation of diaminonaphthalene, 2,6-diethyl carboxylate, followed by a reaction with corresponding metal salts. The octahedral geometry was assigned to both tetraazamacrocyclic complexes as established by electronic measurements. Cyclic voltammetric studies demonstrate intriguing results regarding the stability of their unique oxidation states. The heterogeneous electron transfer rate constant and diffusion coefficient were also computed for two tetraazamacrocyclic complexes and found to be in the range of 1.5×10^{-3} (cm/s) and 1.5×10^{-6} (cm^2/s). The complexes were shown to have better antimicrobial activities against Gram +ve and Gram -ve microorganisms when compared with standard drugs.

Acknowledgments

The author is grateful to Department of Chemistry, GLA University, Mathura, India for all kind of support in this study.

Declarations of interest

The author declares no conflict of interest.

REFERENCES

[1] Y.A. Adebisi, N.D. Jimoh, I.O. Ogunkola, T. Uwizeyimana, A.H. Olayemi, N.A. Ukor, and D.E. Lucero-Prisno, Tropical Medicine and Health 49 (2021) 1.

[2] M. Ferri, E. Ranucci, P. Romagnoli, and V. Giaccone, Critical Reviews in Food Science and Nutrition 57 (2017) 2857.

[3] E. Khan, M. Hanif, M.S. Akhtar, Reviews in Inorganic Chem. 42 (2022) 307.

[4] M. Rezaeivala, and H. Keypour, Coordination Chem. Rev. 280 (2014) 203.

[5] E. Marsault, and M.L. Peterson, J. Medicinal Chem. 54 (2011) 1961.

[6] M.S. More, P.G. Joshi, Y.K. Mishra, and P.K. Khanna, Materials Today Chem. 14 (2019) 100195.

[7] P. Mishra, P. Sethi, S. Kumar, P. Rathi, A. Umar, R. Kumar, S. Chaudhary, A.A.M. Alkhanjaf, A.A. Ibrahim, and S. Baskoutas, J. Mol. Structure (2024) 139098.

[8] S. Srinivasan, P.R. Athappan, and G. Rajagopal. Transition Met. Chem. 26 (2001) 588.

[9] J. Liu, T.B. Lu, H. Deng, and L.N. Ji. Transition Met. Chem. 28 (2003) 116.

[10] Y.G. Fang, J. Zhang, S.Y. Chen, N. Jiang, H.H. Lin, Y. Zhang, and X.Q. Yu. Bioorg. Med. Chem. 15 (2007) 696.

[11] X.Y. Wang, J. Zhang, K. Li, N. Jiang, S.Y. Chen, H.H. Lin, Y. Huang, I.J. Ma, and X.Q. Yu. Bioorg. Med. Chem. 14 (2006) 6745.

[12] D.M. Kong, J. Wang, L.N. Zhu, Y.W. Jin, X.Z. Li, H.X. Shen, and H.F. Mi. J. Inorg. Biochem. 102 (2008) 824.
[13] N. Sengottuvelan, D. Saravanakumar, and M. Kandaswamy, Polyhedron 26 (2007) 3825.
[14] S. Arulmurugan, H.P. Kavitha, and B.R. Venkatraman, Rasayan J. Chem. 3 (2010) 385.
[15] N. Nishat, M.M. Haq, T. Ahamad, and V. Kumar, J. Coord. Chem. 60 (2007) 85.
[16] D.P. Singh, R. Kumar, and J. Singh, Eur. J. Med. Chem. 44 (2009) 1731.
[17] D.P. Singh, R. Kumar, and J. Singh, J. Enzyme Inhib. Med. Chem. 24 (2009) 88.
[18] N. Nishat, and A.S. Dhyani, J. Coord. Chem. 62 (2009) 3003.
[19] P.G. Avaji, and S.A. Patil, J. Enzyme Inhib. Med. Chem. 24 (2009) 140.
[20] S. Chandra, S. Verma, U. Dev, and N. Joshi, J. Coord. Chem. 62 (2009) 1327.
[21] S. Hajari, H. Keypour, M.T. Rezaei, S.H.M. Farida, and R.W. Gable, J. Mol. Structure 1251 (2022) 132049.
[22] H. Zeynali, H. Keypour, L. Hosseinzadeh, and R.W. Gable, J. Mol. Structure 1244 (2021) 130956.
[23] V. Pushpanathan, S.S.J. Dhas, and D.S. Kumar, Chemical Physics Impact 7 (2023) 100264.
[24] M.A. Malik, S.A. Khan, and S.A. Al-thabaiti, Polycyclic Aromatic Compounds 41 (2021) 1431.
[25] N. Sengottuvelan, D. Saravanakumar, and M. Kandaswamy, Inorganic Chem. Commun. 8 (2005) 297.